B. TECH. PROJECT REPORT

On

Performance Analysis of Thermochemical Energy Storage Device for Solar Thermal Applications

BY

Adithyan Kannaiyan
Jagrut Nemade
Raviraj Awasthi

DISCIPLINE OF MECHANICAL ENGINEERING
INDIAN INSTITUTE OF TECHNOLOGY INDORE
NOVEMBER 2017

Performance Analysis of Thermochemical Energy Storage Device for Solar Thermal Applications

A PROJECT REPORT

Submitted in partial fulfillment of the requirements for the award of the degree

of
BACHELOR OF TECHNOLOGY
in

MECHANICAL ENGINEERING

Submitted by:
Adithyan Kannaiyan Jagrut Nemade Raviraj Awasthi

Guided by:
Dr. E. Anil Kumar
Associate Professor, IIT Tirupati

Dr. Devendra Deshmukh
Associate Professor, IIT Indore

INDIAN INSTITUTE OF TECHNOLOGY INDORE
NOVEMBER 2017

CANDIDATE'S DECLARATION

We hereby declare that the project entitled **"Performance Analysis of Thermochemical Energy Storage Device for Solar Thermal Applications"** submitted in partial fulfillment for the award of the degree of Bachelor of Technology in **Mechanical Engineering** completed under the supervision of **Dr. E. Anil Kumar, Associate Professor, Mechanical Engineering,** IIT Tirupati and **Dr. Devendra Deshmukh, Associate Professor, Mechanical Engineering,** IIT Indore is an authentic work.

Further, we declare that we have not submitted this work for the award of any other degree elsewhere.

Adithyan Kannaiyan **Jagrut Nemade** **Raviraj Awasthi**

CERTIFICATE by BTP Guide

It is certified that the above statement made by the students is correct to the best of my knowledge.

Dr. Devendra Deshmukh
Associate Professor
HOD, Department of Mechanical Engineering
IIT Indore

Preface

This report on "**Performance Analysis of Thermochemical Energy Storage Device for Solar Thermal Applications**." is prepared under the guidance of **Dr. E. Anil Kumar and Dr. Devendra Deshmukh**.

In this report, we present a prototype sorption based energy storage device, and we evaluate its performance for different operating conditions. Since its final use is intended to be for solar thermal energy storage, a range of temperatures have been simulated and the corresponding storage capacities and rates have been discussed. The device presented, with more enhancements, could prove fruitful in realizing long term thermal energy storage in the future. We remain hopeful that the data presented herein will remain a useful baseline against which future models could be compared.

Adithyan Kannaiyan, Jagrut Nemade, Raviraj Awasthi

B.Tech. IV Year

Discipline of Mechanical Engineering

IIT Indore

Acknowledgements

We wish to thank **Dr. E. Anil Kumar** and **Dr. Devendra Deshmukh** for his kind support and guidance. We would also like to thank Mr. Rakesh Sharma, Mr. Dharmendra Panchariya and Mr. Dhananjay Mishra of the Heat Transfer Laboratory for their patience and understanding in the workspace and for their valuable insights and design ideas, many of which have found their way into our final work. We extend our gratitude to the Fluid Mechanics and Machinery Laboratory and Mr. Arun Bairwa, who were indispensable in maintaining our workflow. We would like to thank Mr. Anand Petare, Mr. Rishiraj Chouhan and Mr. Satish for their support with Central Workshop equipment. Finally, it would be remiss of us to forget Mr. Ashwin Wagh for his help in financial and administrative matters.

Without their help, this project would not be what it is today.

Adithyan Kannaiyan, Jagrut Nemade, Raviraj Awasthi

B.Tech. IV Year

Discipline of Mechanical Engineering

IIT Indore

Abstract

The present study employs the use of sorption properties of ammonia over Manganese Chloride to develop and test a prototype capable of storing solar energy for long periods (of the order of months). Desorption enthalpy of ammoniated salt ($MnCl_2 \cdot 6NH_3$) is provided by the heat source (heat transfer fluid) with a thermostatic bath maintaining its temperature. Previous research has indicated that the average adsorption and desorption enthalpies for $MnCl_2$ and NH_3 are 65.62 kJ and 60.17 kJ per mole of ammonia in the temperature range of 100-130 °C [1]. However, since these characterizations have been performed using small quantities of salt, these values do not reflect possible energy losses in larger reaction vessels of practical significance. The focus of the present work has thus been to study the performance of such a practical system. Adsorption is carried out under isobaric conditions for pressures ranging from 6 bar to 9 bar. Desorption is carried out at different heat source temperatures, ranging from 100°C to 130°C. Evolution of pressure and temperature are plotted over time. Power delivered and efficiency of the energy storage device are calculated.

Table of Contents

List of Figures

List of Tables

Chapter 1

Introduction

1.1 Energy storage

With an ever increasing demand for energy resulting from both rapidly industrializing countries such as India and China as well as a rising global population, prospects for sustainable power while depending on conventional fossil fuels are bleak. Coupled with a pressing need for a response to global climate change, this rising energy demand has greatly driven forward research in renewable energies and alternative energy sources over the past few decades. In fact, world energy consumption, as measured by Total Primary Energy Supply (TPES), has increased from 70.95 PWh in 1973 to 147.90 PWh in 2010, and its measure in 2015 had increased to 158.7 PWh [2] [3]. At the same time, capacity for renewable energy generation has also steadily risen, though the percentage contribution of alternative sources (including energy from nuclear power, hydro power, biofuel/waste, geothermal, solar, wind, and tidal sources) has risen but little. From 1973 to 2010, the contribution of these alternative sources has increased from 9.44 PWh to 27.95 PWh, and the corresponding percentage contributions to TPES are 13.3% and 18.9% respectively [3]. However, an important observation to be made here is the growth of each alternative source -- since 2010, global nuclear and biofuel capacity have nearly saturated, whereas the contribution from hydro, solar and wind energies has been steadily on the rise. Of these, solar energy seems best poised to see great reduction in costs and increased installation in the near future, since solar energy-based power generation can be scaled in size with ease, unlike in the case of wind and hydro power.

The currently installed solar energy infrastructure has largely been developed over the last 15 years, with a capacity of around 100 GW in 2004 having grown to 667 GW as of 2015. Of this total capacity, 435 GW are utilised by solar thermal heating and cooling equipment, while about 227 GW capacity is contributed by solar PV installations [4]. Thanks to a recent slump in the cost of solar panels, PV installations have enjoyed a faster growth rate than other solar energy storage methods of late. Similarly, a significant improvement in the performance of solar thermal energy storage and conversion techniques could revitalise the growth of solar thermal heating and cooling installations. Particularly in regions where strong sunlight is only seasonally available, energy storage will go a long way in increasing the utilisation of solar energy.

1.2 Methods of thermal energy storage

Thermal energy storage can be classified primarily as sensible heat storage, latent heat storage and thermochemical storage [5]. In sensible heat storage, thermal energy is stored as an increase in the temperature of a material, typically water, earth, or brick (a 'good' material should have a high specific heat capacity, as that translates to a high energy storage density). This, however, is not a viable method for the long term storage which is useful for solar energy applications. Latent heat storage, on the other hand, utilises the phase change of materials (typically water, wax or molten salt) to store energy. While this method provides a higher energy storage density than sensible heating, it still has a few drawbacks -- here too, the subcooling of the material during the phase change process presents a significant energy loss, and phase segregation in the case of hydrated salts results in continuously decreasing performance [6].

Thermochemical heat storage involves either reversible chemical reactions or sorption processes, both of which involve large amounts of energy. In a sorption process, energy is stored in the 'desorption' process, where binding forces between a sorbent and a sorbate are broken, and energy is released in the adsorption or absorption process. Since these processes often involve large enthalpies of reaction, sorption storage systems can offer very high energy storage densities [7].

1.3 Sorption: Terminology and definitions

The IUPAC defines ***adsorption*** as "the enrichment or depletion of one or more components in an *interfacial layer*", where ***interfacial layer*** is in turn defined as "the region of space comprising and adjoining the phase boundary within which the properties of matter are significantly different from the values in the adjoining bulk phases". ***Absorption***, on the other hand, is defined as the "transfer of a component from one phase to the other" [8]. However, since it is often difficult to distinguish between the two processes, and since they sometimes occur simultaneously, the term ***'sorption'*** is commonly used as an umbrella term for all processes involving adsorption and absorption. Within this report, the term ***sorption*** is used to refer to the phenomenon of adsorption described above; the term ***adsorption*** itself is reserved to refer to the process in which molecules accumulate in the interfacial layer, and the term ***desorption*** to refer to the reverse process viz. decrease in the the amount of accumulated molecules, unless explicitly specified.

Particularly in the case of solid-gas adsorption phenomena, the solid phase on which the gas molecules are adsorbed is called the ***adsorbent***. Strictly speaking, the gaseous species in its adsorbed state ought to be

referred to as the ***(ad)sorbate***, and the bulk gaseous phase capable of being adsorbed as the ***(ad)sorptive***. However, since much of today's academic literature dealing with sorption heating/cooling and storage refer to the gas phase as *adsorbate* for simplicity, this report shall do the same [9].

Sorption working pairs mostly boil down to the following types, depending on the interacting phases in the interfacial layer: *solid/gas, solid/liquid, liquid/liquid,* and *liquid/gas*. Within solid/gas pairs, it is necessary to make a distinction between ***chemisorption*** and ***physisorption***. Essentially, when the forces between the different components are valence forces such as those constituting chemical bonds, the phenomenon is called *chemisorption,* while in *physisorption*, the forces involved are Van der Waals forces. While there are a few differences in the properties of the two types of phenomena, the heat of adsorption/desorption is generally the major distinguishing feature; since chemisorption involves the formation and breaking of chemical bonds far stronger than Van der Waals forces, the heat of adsorption/desorption is generally much larger in the case of chemisorption.

1.4 Literature review of sorption systems

Sorption based systems, particularly those utilising solid/gas adsorption and liquid/gas absorption, have been widely studied and characterized. In 2004, the Energy Research Centre of the Netherlands (ECN) conducted an extensive study of potential materials that could be used to store solar heat seasonally, where they identified $MgSO_4/H_2O$ as a particularly promising pair in terms of energy density. At the same time, the Solar Energy Research Centre (SERC) in Netherlands studied the performance of a closed three phase absorption cycle using LiCl/LiCl solution/H_2O with multiple field installations in collaboration with ClimateWell, but it was eventually concluded that it held more promise for solar powered cold storage rather than long term heat storage. In Switzerland, the Institut für Solartechnik SPF (Solartechnik Prüfung Forschung) designed a prototype storage device to investigate the storage properties of zeolites/H_2O and silca gel/H_2O [10]. de Boer et al. (ECN) also characterised the properties of the Na_2S/H_2O chemisorption system [11].

There has also been considerable effort put into developing new generation porous materials for higher H_2O uptake, such as Metal Organic Frameworks (MOFs), Aluminophosphates (AlPOs), and Silico-aluminophosphates (SAPOs), capable of greater adsorption capacities than regular materials [12] [13] [14]

[15] [16]. Recently, composite materials comprised of a salt and a porous matrix have also generated interest since they show higher energy density and better physical properties than regular adsorption pairs [17] [18] [19] [20].

Though adsorption materials have been studied for over a decade now, not many energy storage systems utilising them have been developed. The most prominent examples include:

1) **MODESTORE** (Modular High Energy Density Heat Storage), developed in Austria by the AEE-Intec (Institute for Sustainable Technologies) [21], which used silica gel/H_2O as the working pair
2) **ITW Monosorp**, University of Stuttgart, using zeolite/H_2O as the working pair [10]
3) **MCES** (Modular Chemical Energy Storage) developed at Chiang Mai University, Thailand, using the Na_2S/H_2O chemisorption pair [22]
4) **SWEAT** (Salt-Water Energy Accumulation and Transformation) project, developed at ECN by Boer et al., which also uses the Na_2S/H_2O chemisorption reaction [23]

Apart from these, Zondag et al. at ECN have also developed a prototype thermochemical heat storage system using $MgCl_2/H_2O$ as the working pair [24].

Since in the project described in this report, we have chosen to work with $MnCl_2/NH_3$ as the working pair, previous literature involving ammoniated salt/ammonia pairs is described here. Ammoniate/ammonia pairs have long been studied and used in sorption cooling and heat transformer applications [25] [26], but their use in thermal energy storage has received attention only in recent years. In 2012, Li et al. proposed an sorption system for integrated energy storage and upgrade [27], using a combined system of 2 solid/gas reactors using ammoniated salt/ammonia and a refrigerant vessel, while more recently, in 2016, they proposed a multilevel sorption thermal battery for solar energy storage [28]. In the latter, the proposed system operates a solid/gas adsorption reactor filled with various reactant materials as well as a liquid tank for liquid/gas absorption with the working gas circulating between the two. The system shows a wide operating range of temperatures, which is useful given the variation of solar energy availability, and they report energy densities of up to 1200 kJ/kg based on their calculations. Sakamoto and Yamamoto have developed and studied a thermochemical energy storage unit using $CaCl_2/NH_3$ as the working pair, discussed the volume expansion and salt activity over repeated cycles, and have also investigated the effect of mixing titanium metal with salt on the reaction

time for adsorption and desorption reactions [29] [30]. In 2017, Sharma and Anil Kumar performed experiments to characterize the sorption thermal properties of $CaCl_2$, $SrCl_2$, $MnCl_2$, and $FeCl_2$ [1] . Based on the Van ‘t Hoff plot they obtained from their experiments, the adsorption and desorption enthalpies for these salts (in the order they were listed) were found to be 44.01/56.59, 54.32/66.60, 60.17/65.62 and 66.87/92.99 kJ/mol of ammonia respectively. However, significant losses may be expected in a prototype or full scale sorption storage system, where the mass of the reactor vessel entails a significant sensible heat loss.

Chapter 2

Experimental Setup and Reactor Design

2.1 Experimental Setup

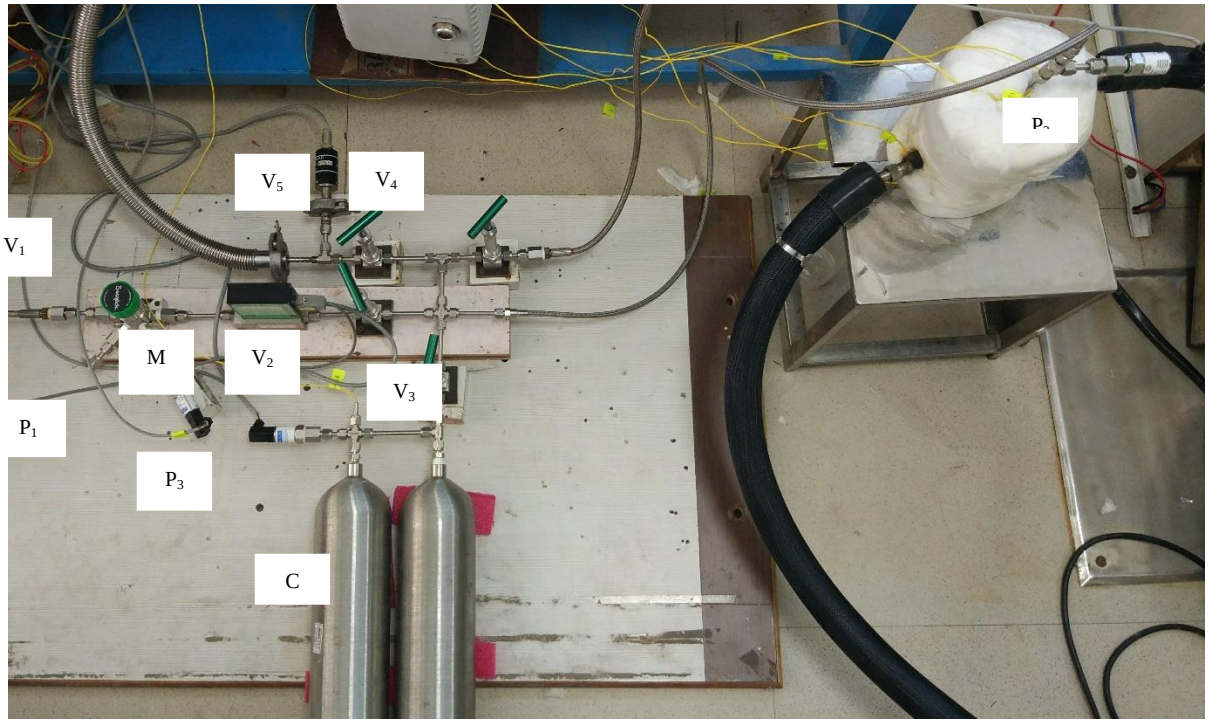

Figure 2.1: Experimental setup.

The gas flow setup consists of mainly following components as shown in Figure 2.1. The description of the various components used in the setup are explained below.

2.1.1 Pressure Regulator

It is a Swagelok Compact General Purpose Diaphragm-Sensing Back-Pressure Regulator. It is used mainly to maintain the upstream pressure control in the setup. The pressure control range for this regulator is from 0 bar to 34.4 bar [31]. It has four ports, two for high pressure inlets and two for low pressure outlets.

2.1.2 XFM Mass Flow Meter

Mass Flow Meter helps to keep check on the flow of ammonia. It records the flow rate in g/sec and the totalizer is updated accordingly. The stream of gas entering the Mass Flow transducer is split by shunting a small portion of the flow through a capillary stainless steel sensor tube. The remainder of the gas flows through the primary flow conduit. The geometry of the primary conduit and the sensor tube are designed to ensure laminar flow in each branch. According to principles of fluid dynamics, the flow rates of a gas in the two laminar flow conduits are proportional to one another. Therefore, the flow rates measured in the sensor tube are directly proportional to the total flow through the transducer. In order to sense the flow in the sensor tube, heat flux is introduced at two sections of the sensor tube by means of precision-wound heater sensor coils. Heat is transferred through the thin wall of the sensor tube to the gas flowing inside. As gas flow takes place, heat is carried by the gas stream from the upstream coil to the downstream coil windings. The resultant temperature dependent resistance differential is detected by the electronic control circuit. The measured temperature gradient at the sensor windings is linearly proportional to the instantaneous rate of flow taking place. An output signal is generated that is a function of the amount of heat carried by the gases to indicate mass molecular based flow rates [32].

2.1.3 Pressure Transducers

They are used to measure pressures at various points in the setup. They are connected to the Data Acquisition (DAQ) System. The ranges of the pressure transducers used in the setup are 0 to 25 bar, 0 to 50 bar and 0 to 200 bar and the voltage output range is 0 to 10 V. Thus, there is a linear variation between the output voltage and the pressure with slope being 2.5, 5 and 20 respectively.

2.1.4 Needle Valves

Swagelok Needle Valves are used to allow or restrict the flow of fluids. The working pressure is up to 413 bar and it is compatible with fluids whose temperatures lie between -28 ºC and 343 ºC [33]. The valves in this setup are placed in such a way that the flow of gas during adsorption and desorption is taken care of without letting the ammonia enter the cylinders C during adsorption and without letting the ammonia flow towards MFM during desorption.

2.1.5 Thermostatic Bath

JULABO FP50-HL Refrigerated/Heating Circulator is used as a thermostatic bath for the adsorption and desorption experiments. The fluid which is used to circulate inside the reactor is Thermal H10. The working temperature range for this thermostatic bath is -50 ºC to 200 ºC. The temperature stability for this device is ± 0.01 ºC. The pump capacity flow rate varies from 22 L/min to 26 L/min [34]. The heat transfer fluid (Thermal H10) is circulated through the reactor using heavily insulated pipes.

2.1.6 Thermocouples

Type K thermocouples are used in this setup. Further, probe type and bead type thermocouples are used for various purposes. They are connected to the Data Acquisition (DAQ) System. Probe type thermocouples are used to measure the temperature within the reactor and within the cylinders C. Bead type thermocouples are used to measure the inlet and outlet temperatures of the fluid jacket surrounding the salt bed.

2.1.7 Data Acquisition (DAQ) System

Measurements provided by Pressure Transducers and Thermocouples are recorded using a DAQ and are directly saved into a computer for further study. The Agilent Technologies 34970A is used to perform data storage, data reduction, mathematical calculations, and conversion to engineering units. You can use the PC to provide easy configuration and data presentation [35]. There are 20 two-wire channels to which you can connect the entity such as a pressure transducer or a thermocouple.

2.2 Reactor Design

A Thermochemical energy storage device is designed for the sorption experiments. As shown in Figure 2.2 and Figure 2.3, there are various modules involved in the design of the reactor. The centermost entity is a gas diffuser through which ammonia gets diffused into the salt surrounding it. Here, the salt used is anhydrous Manganese Chloride ($MnCl_2$). The salt is prepared and activated as mentioned in the next chapter. The salt bed is surrounded by 10 mm thick SS316 wall beyond which the Heat Transfer Fluid flows. This fluid is circulated at lower temperature for adsorption cycle and at higher temperatures during desorption cycle. This fluid jacket is connected to the thermostatic bath. Four Thermocouples are inserted

in the salt bed, two of them are near the diffuser at different heights and the other two are near the wall at those heights. These thermocouples serve the purpose of ensuring that the gas diffusion is constant along the length and to ensure that the entire salt bed is at same temperature while the reaction takes place. Two bead type thermocouples are present at the inlet and outlet of the HTF jacket. The reactor is insulated with glass wool to avoid unnecessary heat losses from the HTF to the atmosphere. A piece of glass wool is kept at the bottom of the salt bed to avoid heat transfer in the axial direction.

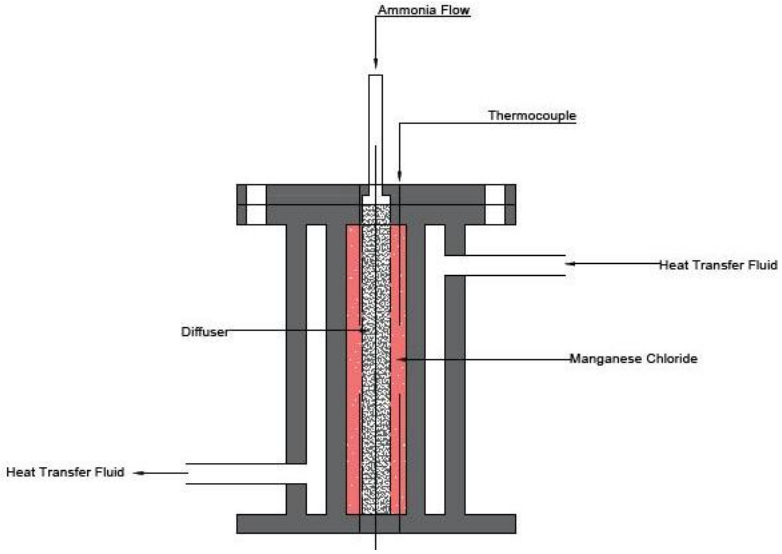

Fig. 2.2. Reactor Design

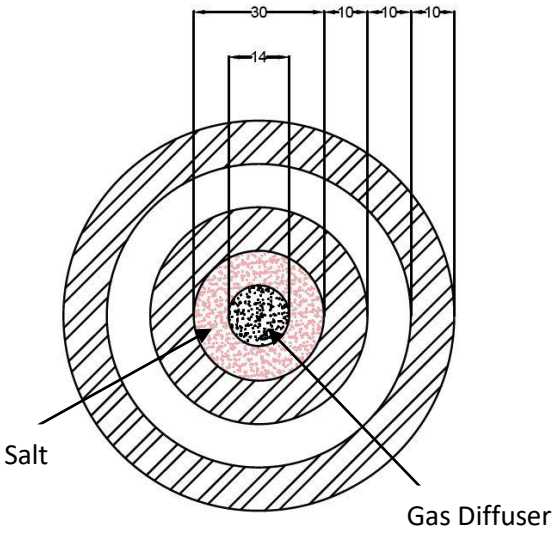

Fig. 2.3. Top view of the reactor[1]

[1] All dimensions are in mm.

Chapter 3

Experimental Approach

3.1 Leak Test

The gas used in the adsorption and desorption experiments of $MnCl_2$ is ammonia (NH_3). To ensure that this gas is transferred from the gas cylinder to the reactor without any loss to atmosphere, leak test is carried out. Gas leaks can occur due to loose tightening of nuts, fault in components involved in the setup such as pressure regulators, pressure transducers, and hoses.

To ensure if the setup is leak-proof, SNOOP® Liquid Leak Detector was used. This liquid leak detector, when dripped over joints or junctions, developed bubbles if there was a presence of any leak. This leak can be fixed by further tightening of the nut or replacement of the specific component.

The gas used for the leak test was Argon (Ar) as it is an inert gas which won't react with the salt, and in case of any leak, it is not harmful unlike NH_3. Argon was passed through the setup at 16 bar. Leaks were found at few joints, which were fixed using one of the aforementioned methods. Constant pressure of 16 bar was obtained which was measured using a pressure transducer. Thus, there were no further leaks.

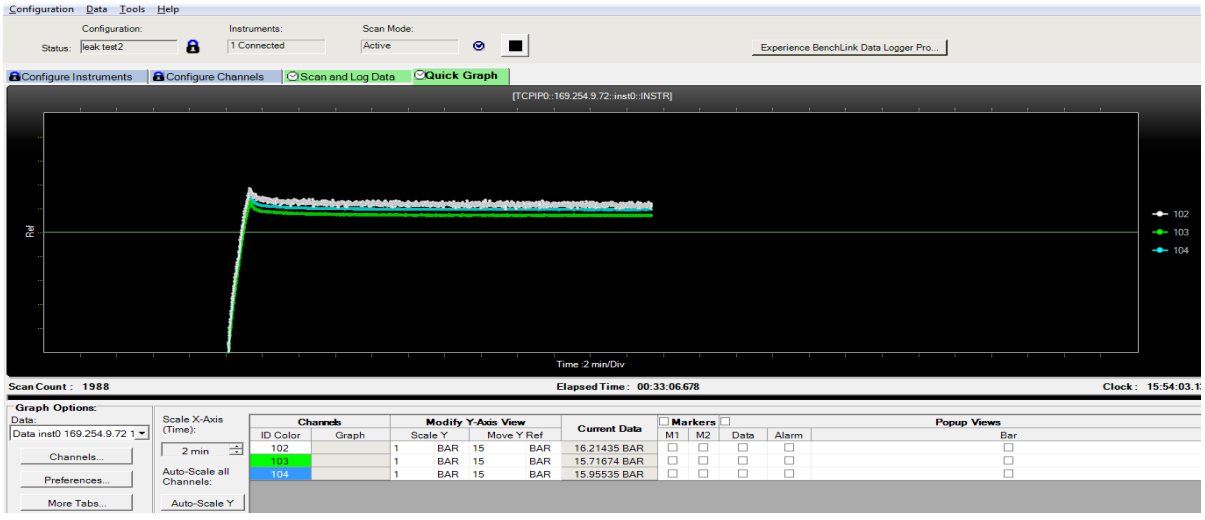

Figure 3.1. Leak test at 16 bar

This leak-proof setup was then ready for the further experiments using NH_3.

3.2 Salt Preparation

Anhydrous manganese chloride has a high affinity towards water thereby exhibiting a tendency to get readily hydrated once exposed to the atmosphere. However to perform the sorption of ammonia, the salt needs to be free of any impurity which could possibly reduce the adsorption capacity of the salt itself. Therefore initial preparation of the salt is required before it is put inside the reactor for purpose of testing.

A measured amount of hydrated manganese chloride was dried in a vacuum oven at a temperature of 120 °C and a vacuum pressure of 560 mm of Hg for a period of 5 hours. The anhydrous salt obtained was measured on a weighing machine and the mass of the anhydrous salt was recorded. The mass of salt before and after the dehydration process was measured to be 150 gm and 104 gm respectively. The above measured mass values indicates a significant amount of water being present in the salt therefore making dehydration an essential part of salt preparation process.

The prepared salt was filled in the reaction chamber using a spatula with the gas diffuser in its position and was compacted using a glass rod for accommodating more salt inside the reaction chamber. The amount of salt leftover was again measured and was found to be 23 gm. Special care was taken that no salt got wasted during the filling operation.

Based upon the measured values of salt obtained after the filling operation, 81 gm of anhydrous $MnCl_2$ was estimated to be present in the reaction chamber.

3.3 Salt Activation

Though dehydration of salt had already been performed, there was a possibility of the presence of oxide impurities present in the salt which could have significantly reduced the ammonia adsorbing capacity of $MnCl_2$. Therefore, in order to remove such impurities various adsorption-desorption cycles were run at highest possible adsorption pressure (9 bar) and highest possible desorption temperature (130 °C) respectively. The continuous adsorption-desorption cycle increases the exposure of salt with ammonia thereby accounting for more ammonia adsorption capacity of the salt.

Ammonia was adsorbed over the salt at a constant supply pressure of 9 bar while maintaining the temperature of the salt bed at 15 °C using the JULABO thermostatic bath. The mass of ammonia flown

through the digital mass flow meter XFM37 was recorded each time once the value of mass flow rate reached 0.00 g/s through it.

Following the adsorption process, desorption of ammonia was performed at high temperatures (140 °C) to remove the impurities present in the salt along with the ammonia and also to make the salt ready for further adsorption-desorption cycles.

Each desorption cycle was succeeded by vacuuming of the entire reaction chamber to a vacuum pressure of 1.5 mbar such that a completely desorbed salt bed with a minimal amount of impurities is present for further activation process.

Mentioned below are the mass flow meter readings observed for successive activation cycles:

Experiment No.	Mass flow meter reading (gm)
1.	9.6
2.	12.5
3.	17.4
4.	22.1
5.	27.5
6.	31.8
7.	32.3
8.	32.1

Table 3.1. Salt activation

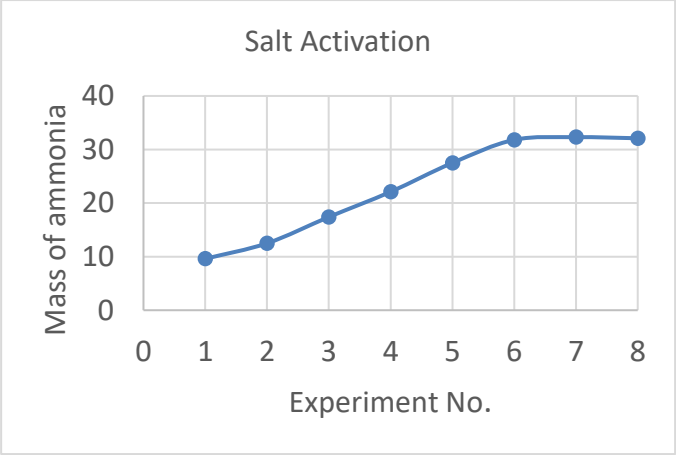

Fig. 3.2. Mass of ammonia vs experiment no.

The curve in the Fig. 3.2 shows a steady adsorption capacity of the salt after the fifth experiment with an average value of 32 gm. These observations indicated that the salt had reached its saturation state and no more ammonia could be adsorbed over it by conducting further activation cycles.

A maximum of 39.6 wt % of ammonia was adsorbed over the salt at 9 bar and the salt bed temperature of 15 °C.

3.4 Experimental Procedure

The preceding section over the description of the experimental setup briefly explains the presence of the different needle valves leading to different outlet ports. However, it was the opening and closing of these valves that decided the conditions under which a particular reaction was performed.

In the present experimental analysis and performance testing of the device, sorption reactions were carried out under different sets of conditions. The discharging (or adsorption) of the device was carried out under constant supply pressure of ammonia while, the charging or desorption was performed for a constant temperature of the heat source.

Before performing any sorption cycle, removal of atmospheric impurities from the reaction chamber and the calibrated cylinders was essential. To achieve this, the salt was heated to a temperature of 140 °C using the heat transfer fluid, while the entire setup (reaction chamber and the cylinders) was connected to the vacuum pump by opening the vacuum valve. The process was continued until the pressure inside the setup reached 1.5 mbar as measured by the Pirani gauge.

During the above mentioned procedure, the valve to the exhaust was closed to avoid any air getting sucked into the reaction chamber. The valve connecting the reaction chamber to supply cylinder was also kept closed to avoid any damage to the mass flow meter.

Following the vacuum of the setup, cold heat transfer fluid was supplied through the cooling jacket allowing the salt and the device to cool down before it becomes ready for the adsorption process. Cooling was performed until the temperature of the salt bed reached a steady value of around 15 °C.

Pressure regulator connecting the setup with the supply cylinder was kept closed initially thereby cutting the supply between the high pressure side (supply cylinder) and the low pressure side (reaction chamber) completely. The supply cylinder was opened until the supply pressure as measured by the pressure transducer on the pressure regulator reached the desired adsorption pressure. The inlet temperature of the heat transfer fluid was maintained at 15 °C using the thermostatic bath.

Valves connecting the main gas supply line to the exhaust, vacuum and the calibrated cylinders were closed such that reaction chamber was in series with the main supply cylinder. The mass of ammonia flown to the

reaction chamber was recorded using the digital mass flow meter. The energy released during the adsorption was carried away by the heat transfer fluid in the cooling jacket and its corresponding temperature rise was recorded. Ammonia was supplied into the reaction chamber until the flow rate decreased to 0.00 g/sec as displayed by the digital mass flow meter.

Using the above mentioned procedures, discharging of the device was tested for different adsorption pressures. However in order to perform desorption, it is desirable to have a high concentration of ammonia adsorbed over the salt such that large energy storage density could be achieved. Moreover using one adsorption pressure serves as a reference for the concentration of ammonia over the salt bed taken for desorption at different temperatures. This basically helps us in making a comparison study for different desorption temperatures for a particular adsorbed salt bed.

Therefore in order to achieve this, after the adsorption was completed, the ammonia was supplied at the maximum possible pressure (9 bar). Maximum possible adsorption over the salt bed was allowed to happen before proceeding for the desorption reactions.

Desorption of the salt bed was carried out by passing the heated heat transfer fluid through the fluid jacket. The inlet to the fluid jacket was maintained at a constant temperature while the corresponding temperature drop of the fluid at the outlet was measured. The energy lost by the heat transfer fluid corresponded to the energy stored in the salt and the sensible heat loss during the charging. Valves connecting the reaction chamber to the vacuum, exhaust and the supply cylinder were kept closed. The desorbed ammonia was collected in the calibrated cylinders and its corresponding pressure and temperature was recorded. Experiment was recorded until the temperature difference of the heat transfer fluid between inlet and outlet of the fluid jacket became negligibly small.

After the completion of desorption, the salt bed was again heated to a temperature of 140 °C in order to facilitate the complete desorption of the salt bed and make it ready for the next sorption cycle.

Chapter 4

Results and Discussion

The main objective of the device was to store the thermochemical energy and release it whenever required. Therefore special emphasis was put upon the amount of energy that could be stored in the salt during desorption and the energy that could be released due to adsorption under different operating conditions. Moreover, the amount of ammonia involved during each sorption process was also studied to analyze the behaviour of the salt.

Overall energy input/output was calculated by integrating the instantaneous energy transfer to the fluid given by the equation below:

$$\boldsymbol{q = mc\Delta T}$$

Where q denotes the energy transfer rate, m being the mass flow rate, c being the specific heat capacity, ΔT being the temperature change of the heat transfer fluid.

4.1 Adsorption (Discharging)

With the variation of supply pressure during adsorption, an adsorption plateau was found to exist for the supply pressure ranging from 6-8 bar and a salt bed temperature of 15 °C. During this plateau, the weight percentage of ammonia adsorbed was found to be fairly constant. However, a sudden increase in this value was observed as the pressure was changed to 9 bar indicating the end of the adsorption plateau. The weight concentration of ammonia over the salt during the adsorption plateau was found to be near 24%, while the value increased to 34% once the pressure was increased to 9 bar.

A similar behavior in the energy output was also observed justifying the above observation. The salt bed temperature reached its maximum value within first few seconds of the adsorption but then decreased continuously till the end of the reaction. Therefore the instantaneous power was observed to be maximum within the first few seconds of the adsorption and then decreased as the discharging progressed. The maximum instantaneous power as well as the average output power was found to be increasing with the increase in the adsorption pressure. The experimental observations and the results during adsorption are mentioned in the table below:

Supply Pressure (bar)	Ammonia Adsorbed (gm)	Energy Released (kJ)	Average Output Power (W)
6	19.4	112.62	94
7	19.6	115.41	111
8	20.4	128.01	115
9	27.8	156.95	134

Table 4.1. Adsorption Characteristics

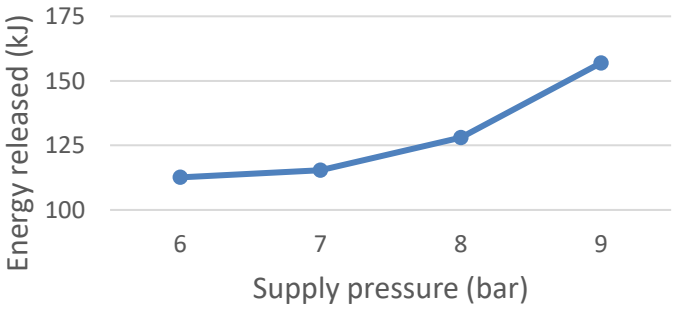

Fig. 4.1 Energy vs Pressure

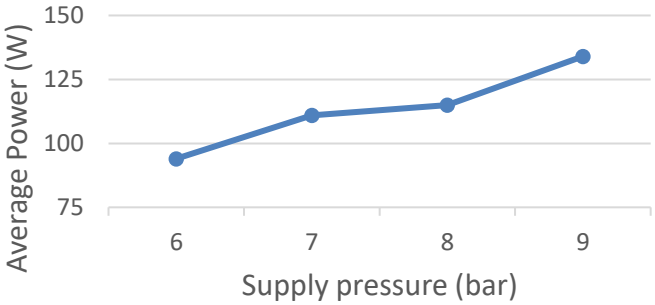

Fig. 4.2. Average Power vs Pressure

4.2 Desorption (Charging)

During desorption the energy transferred to the salt bed from the heat transfer fluid was calculated using the above mentioned equation. However, a significant portion of this overall energy transfer was lost during the sensible heating of the steels walls of the device itself. However, energy storage density as high as 3.3 kJ/gm of salt was achieved at a charging temperature of 130 °C.

As the charging temperature was increased, the total energy transfer along with the sensible heat loss and the energy stored in the salt were found to increase. Maximum amount of energy that could be stored by the salt

was calculated to be 267.33 kJ. The table given below depicts the performance of the device during charging operation.

Charging Temperature (°C)	Total Energy Stored (kJ)	Sensible Heat Loss (kJ)	Energy Stored in Salt (kJ)	Energy Storage Density (kJ/gm)
100	455.56	262.48	193.48	2.39
110	508.91	295.29	213.62	2.64
120	542.63	328.09	214.54	2.65
130	628.24	360.91	267.33	3.30

Table 4.2. Desorption Characteristics

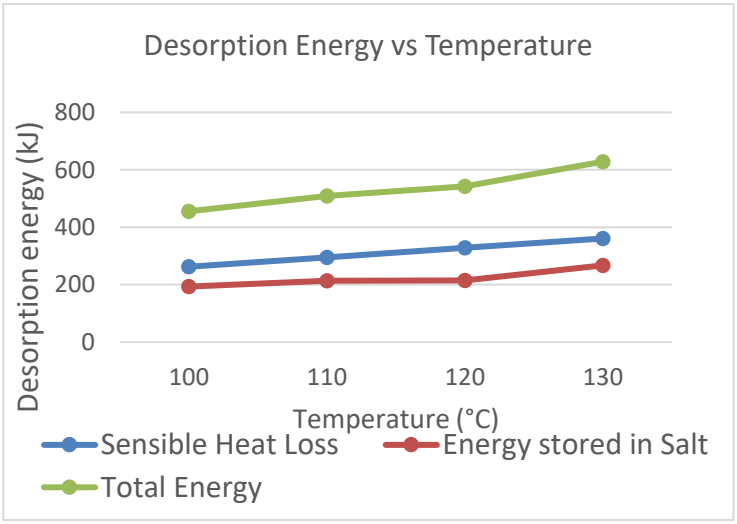

Fig. 4.3. Desorption Energy vs Temperature

4.3 Efficiency

It has already been discussed that the energy stored in the salt was found to increase with the increasing charging temperature. However, it is important that the maximum possible utilization of the stored energy is carried out such very minimal energy losses are observed. Thus, in order to choose the appropriate charging temperature, study of the efficiency of the device under different set of operating conditions becomes an utmost requirement.

As per the experimental observations, the maximum energy released from the salt was obtained at the maximum discharging pressure. Hence a pressure of 9 bar was taken to utilize the salt to the maximum extent. The adsorbed salt bed was charged at different charging temperatures as discussed above and based upon the energy values obtained, the efficiency of the device was calculated. The table below depicts the variation of the device efficiency with various charging temperatures.

S. No.	Charging Temperature (°C)	Efficiency
1.	100	0.344
2.	110	0.308
3.	120	0.289
4.	130	0.250

Table 4.3. Device Efficiency

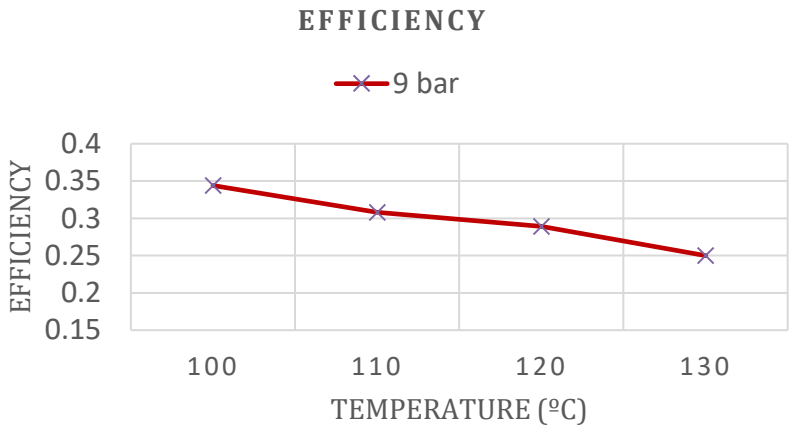

Fig. 4.4. Efficiency vs Temperature

The above drawn curve clearly indicates that the overall device efficiency behaves completely opposite to the energy storage for different charging temperatures. A maximum efficiency of 34.4% was observed for a charging temperature of 100 °C and was found to increase thereafter with the increasing charging temperatures. Thus this results in a trade-off between the maximum energy that could be stored and the device efficiency. Thus based upon the efficiency and the energy requirement, a suitable operating condition for the device could be chosen.

Chapter 5

Conclusions and Further Enhancements

5.1 Conclusion

Based upon the results of the experiments performed, various conclusions could be drawn for different sorption processes. For the desorption process, increasing the charging temperature corresponded to an increase in the energy stored in the salt however compromising with the efficiency of the device. Thus, the clear tradeoff between the energy stored and the device efficiency should always be kept in mind before selecting the optimum charging conditions.

The results of the discharging process basically indicates an increase in power and the energy output with the increasing adsorption pressure. However, the occurrence of the adsorption plateau between 6 bar and 8 bar of ammonia pressure basically indicates a no gain zone wherein significant rise in the energy released cannot be achieved just by increasing the ammonia pressure. Thus a higher pressure (9 bar) is required for more energy output.

5.2 Further Enhancements

The reactor design used in the current project work is only a first prototype designed with a considerable factor of safety in mind. Also, the salt bed was retained in as simple an arrangement in order to establish baseline data against which future work could be compared. Such enhancements include:

- Reduction in metal-mass of the reactor vessel. Since the metallic mass of the reactor is a considerable source of energy loss, a heavier reactor will present a lower efficiency. Thus, the first logical step in attempting to refine the design of the device should be to optimize its weight.

- Sorption reactions generally require a long time to proceed to completion; during adsorption, the increase in temperature favours the reverse reaction, while during desorption, for a closed system, the increase in pressure favours adsorption. In order to enable these reactions to proceed faster, it is necessary to improve the rate of heat transfer from the heat transfer medium to the salt. This can be achieved in a few ways:

- Using metallic fins to improve the effective thermal conductivity. For example, in a simple extension of our existing design, alternating layers of thin fins and salt could be stacked on top of each other.

- By mixing the powdered salt with materials that would enhance the effective thermal conductivity. Carbonaceous materials such as graphite flakes or expanded natural graphite (ENG) may be used for this purpose, as well as powdered metals such as titanium.

Of course, while pursuing these enhancements, we must also keep in mind the increased cost of the resulting material, as well as the fact that a higher proportion of support materials such as fins or carbon results in lesser salt content, and lesser energy density.

- Another possible avenue worth exploring is the use of compressed pellets that would allow for denser packing of the salt. This would, however, decrease the permeability of the salt. It might be possible to offset this drawback by using pellets of salt mixed with ENG in order to increase its pore volume.

References

[1] R. Sharma and A. Kumar, "Performance evaluation of simple and heat recovery adsorption cooling system using measured NH3 sorption characteristics of halide salts," *Applied Thermal Engineering*, pp. 459-471, 2017.

[2] International Energy Agency, "Key World Energy Statistics 2017," 2017.

[3] International Energy Agency, "Key World Energy Statistics 2012," 2012.

[4] REN21, "Renewables 2017 Global Status Report," 2017.

[5] J. Hadorn, "Advanced storage concepts for active solar energy - IEA SHC Task 32," in *Proceedings of First International Conference on solar heating, cooling and buildings*, Lisbon, Portugal, 2008.

[6] M. M. Farid, A. M. Khudhair, S. A. K. Razack and S. Al-Hallaj, "A review on phase change energy storage: materials and applications," *Energy Conversion and Management,* vol. 45, no. 9-10, pp. 1597-615, 2004.

[7] A. Hauer, "Sorption theory for thermal energy storage," *Paksoy H.Ö. (eds) Thermal Energy Storage for Sustainable Energy Consumption. NATO Science Series (Mathematics, Physics and Chemistry),* vol. 234, pp. 393-408, 2007.

[8] D. Everett, "Appendix II: Definitions, Terminology and Symbols in Colloid Surface Chemistry," *Pure and Applied Chemistry,* vol. 31, no. 4, pp. 577-638, 1972.

[9] N. Yu, R. Wang and L. Wang, "Sorption thermal storage for solar energy," *Progress in Energy and Combustion Science,* vol. 39, pp. 489-514, 2013.

[10] C. Bales, "Final report of Subtask B, Task 32: "Chemical and Sorption Storage" the overview," 2008.

[11] R. de Boer, W. Haije and J. Veldhuis, "Determination of structural, thermodynamic and phase properties in the Na2S-H2O system for application in a chemical heat pump," *Thermochimica Acta,* vol. 395, pp. 3-19, 2003.

[12] S. Henninger, H. Habib and C. Janiak, "MOFs as adsorbents for low temperature heating and cooling applications," *Journal of the American Chemical Society,* vol. 131, no. 8, pp. 2776-2777, 2009.

[13] Y. Aristov, "Novel materials for adsorptive heat pumping and storage: screening and nanotailoring of sorption properties," *Journal of Chemical Engineering of Japan,* vol. 40, pp. 1242-51, 2007.

[14] S. Henninger, F. Jeremias, H. Kummer and C. Janiak, "MOFs for use in adsorption heat pump processes," *European Journal of Inorganic Chemistry,* vol. 2012, no. 16, pp. 2625-34, 2012.

[15] D. K. Panchariya, R. K. Rai, S. K. Singh and E. A. Kumar, "Synthesis and characterization of MIL-101 incorporated with Darco type activated charcoal," *Materials Today: Proceedings,* vol. 4, no. 2, pp. 388-94, 2017.

[16] S. Henninger, F. Schmidt and H. Henning, "Water adsorption characteristics of novel materials for heat transformation applications," *Applied Thermal Engineering,* vol. 30, no. 13, pp. 1692-702, 2010.

[17] L. Gordeeva and Y. Aristov, "Composites ‘salt inside porous matrix’ for adsorption heat transformation: a current state-of-the-art and new trends," *International Journal of Low-Carbon Technologies,* vol. 7, no. 4, pp. 288-302, 2012.

[18] Y. Aristov, "Novel materials for adsorptive heat pumping and storage: screening and nanotailoring of sorption properties," *Journal of Chemical Engineering of Japan,* vol. 40, no. 13, pp. 1242-51, 2007.

[19] I. Ponomarenko, I. Glaznev, A. Gubar, Y. Aristov and S. Kirik, "Synthesis and water sorption properties of a new composite “CaCl2 confined into SBA-15 pores”," *Microporous and Mesoporous Materials,* vol. 129, no. 1, pp. 243-50, 2010.

[20] Y. Aristov, M. Tokarev, G. Restuccia and G. Cacciola, "Selective water sorbents for multiple applications, 2. CaCl2 confined in micropores of silica gel: sorption properties," *Reaction Kinetics and Catalysis Letters,* vol. 59, no. 2, pp. 335-342, 1996.

[21] G. Gartler, D. Jähnig, G. Purkarthofer and W. Wagner, "AEE Intec - Institute for Sustainable Technologies," 2004. [Online]. Available: http://projekte.aee-intec.at/0uploads/dateien7.pdf.

[22] K. Iammak, W. Wongsuwan and T. Kiatsiriroj, "Investigation of Modular Chemical Energy Storage Performance," in *The Joint International Conference on “Sustainable Energy and Environment (SEE)”*, Thailand, 2004.

[23] R. de Boer, W. Haije, J. Veldhuis and S. Smeding, "Solid sorption cooling with integrated storage: the SWEAT prototype," in *3rd international heat powered cycles conference—HPC 2004*, Larnaca, Cyprus, 2004.

[24] H. Zondag, B. Kikkert, S. Smeding, R. de Boer and M. Bakker, "Prototype thermochemical heat storage with open reactor system," *Applied Energy,* vol. 109, pp. 360-365, 2013.

[25] P. Neveu and J. Castaing, "Solid-gas chemical heat pumps: field of application and performance of the internal heat of reaction recovery process," *Heat Recovery Systems and CHP,* vol. 13, no. 3, pp. 233-51, 1993.

[26] L. Vasiliev, D. Mishkinis and A. Antukh, "Solar-gas solid sorption refrigerator," *Adsorption,* vol. 7, no. 2, pp. 149-161, 2001.

[27] T. Li, R. Wang and J. Kiplagat, "A target-oriented solid-gas thermochemical sorption heat transformer for integrated energy storage and energy upgrade," *Thermodynamics and Molecular Scale Phenomena, AIChE J.,* vol. 59, pp. 1334-47, 2013.

[28] T. Li, S. Wu, T. Yan, J. Xu and R. Wang, "A novel solid–gas thermochemical multilevel sorption thermal battery for cascaded solar thermal energy storage," *Applied Energy,* vol. 161, pp. 1-10, 2016.

[29] Y. Sakamoto and H. Yamamoto, "Performance of Thermal Energy Storage Unit Using Solid Ammoniated Salt (CaCl2-NH3 System)," *Natural Resources,* vol. 5, pp. 337-342, 2014.

[30] Y. Sakamoto, H. Yamamoto, S. Sanga and J. Tokunaga, "Performance of Thermal Storage Unit Using CaCl2-NH3 System Mixed with Ti," *The Canadian Journal of Chemical Engineering,,* vol. 68, pp. 948-951, 1990.

[31] Swagelok, [Online]. Available: https://www.swagelok.com/en/product/Regulators/Back-Pressure-Spring-Loaded.

[32] Aalborg, [Online]. Available: http://www.aalborg.com/images/file_to_download/en_Aalborg_EM20170915_XFM.pdf.

[33] Swagelok Needles, [Online]. Available: https://www.swagelok.com/en/product/Valves/Needle-Shutoff-and-Regulating.

[34] Julabo, [Online]. Available: https://www.julabo.com/en/products/refrigerated-circulators/refrigerated-heating-circulators/fp50-hl-refrigerated-heating-circulator.

[35] Agilent, [Online]. Available: http://www.me.umn.edu/courses/me4331/FILES/AgilentManual_34.pdf.

Appendix

Calibration

A.1 Mass Flow Meter Calibration

The experiments involved in this project primarily includes adsorption and desorption cycles using Ammonia (NH_3). To keep a record of the amount of ammonia passing through the setup to the reactor, XFM Mass Flow Meter was used.

Fig. A.1. XFM Mass Flow Meter

As shown in Fig. A.1, it displays the instantaneous mass flow rate in g/sec and the totalizer value i.e. the total amount of gas passed through it. The least count of the mass flow rate is 0.001 g/sec while that of the totalizer is 0.1 g. For the calibration of MFM, a setup was built to calculate the mass flowed through the setup.

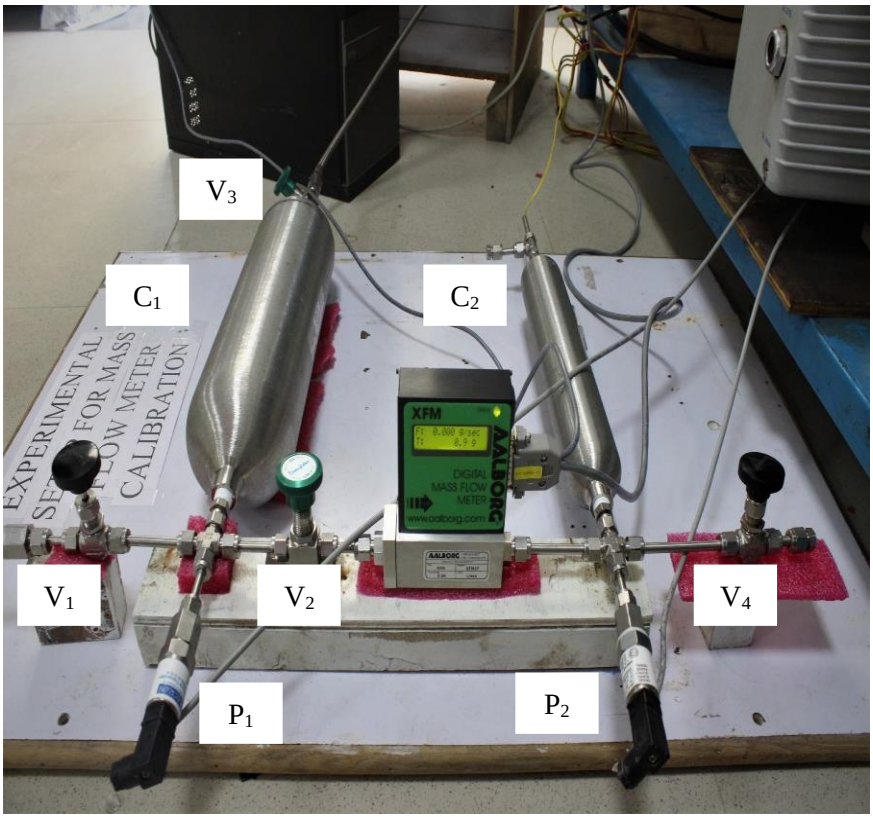

Fig. A.2. XFM calibration setup

The setup consists of two SS316 calibrated cylinders, their volumes being 2250 ml (C_1) and 500 ml (C_2), XFM MFM, two pressure transducers (P_1 and P_2), and valves (V_1, V_2, V_3 and V_4) to restrict and allow the flow of the gas. Leak test has been performed on this setup using Argon gas before beginning the calibration process.

V_4 is kept closed at all times. Ammonia is passed through the MFM at different supply pressures ranging from 4 bar to 9 bar. The two pressure transducers P_1 and P_2 measure the pressures of C_1 and C_2 respectively. V_2 is closed before opening the ammonia gas cylinder. The desired supply pressure can be attained by filling C_1 with ammonia such that the pressure P_1 is equal to or just above the desired supply pressure. V_1 is then closed. In case of excess pressure in C_1, some amount of gas is exhausted from V_3 until the pressure P_1 is equal to the desired supply pressure. The gas is then passed through MFM by opening V_2 and C_2 gets filled with ammonia until both pressures P_1 and P_2 are equal. From P2, amount of ammonia in C2 was calculated and compared with the expected/theoretical amount of ammonia. Following is the data of amount of ammonia at different supply pressures.

Supply Pressure (bar)	MFM Value (g)	Theoretical Value (g)	Error %
4	1.071	1.115	3.94
5	1.292	1.382	6.51
6	1.52	1.64	7.31
7.01	1.844	1.921	4
8.01	2.212	2.24	1.25
9.04	2.545	2.553	0.31

Table A.1. XFM Calibration

From the above data, we can infer that the error in the mass flow meter reading decreases with increase in pressure after 6 bar. The maximum error was found about to be 7.31%.

A.2 Thermocouple Calibration.

Type K thermocouples were used in the experimental setup. Further, two types of Type K thermocouples were used, viz. probe type and bead type.

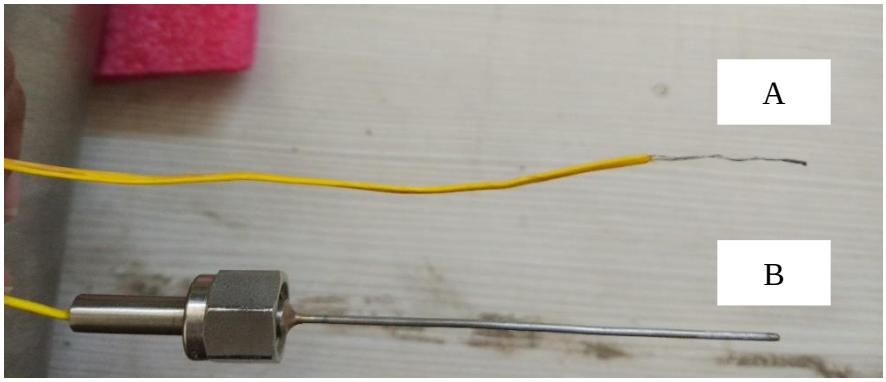

Figure A.3. Thermocouples used (A - Bead type, B - Probe type)

The temperature of the thermostatic bath, JULABO FP50-HL Refrigerated/Heating Circulator was used as reference for calibrating these thermocouples. The thermostatic bath was maintained at different temperatures ranging from 60 ºC to 120 ºC. After the bath reaches each of these temperatures, the thermocouples were inserted in it and the measurements were recorded.

Figure A.4. Thermocouple Calibration

Thermostatic Bath Temperature (ºC)	Probe type (ºC)	Bead type (ºC)
60	60.2	59.2
70	69.5	70.1
80	79.3	79.7
90	89.6	90.2
100	99.8	100.2
110	109.6	109.7
120	119.5	119.9

Table A.2. Thermocouple Calibration

From the above data, we can infer that the maximum deviation between the thermocouple value and the reference value is 0.8 ºC and the tolerance of the thermocouples is ±1%.